Journal of Colloid and Interface Science 432 (2014) 19–25

Contents lists available at ScienceDirect

Journal of Colloid and Interface Science

www.elsevier.com/locate/jcis

Facile and fast synthesis of graphene oxide nanosheets via bath ultrasonic irradiation

A. Esmaeili [a], M.H. Entezari [a,b,*]

[a] Sonochemical Research Center, Department of Chemistry, Ferdowsi University of Mashhad, 91775 Mashhad, Iran
[b] Environmental Chemistry Research Center, Department of Chemistry, Ferdowsi University of Mashhad, 91775 Mashhad, Iran

ARTICLE INFO

Article history:
Received 15 March 2014
Accepted 24 June 2014
Available online 1 July 2014

Keywords:
Facile synthesis
Graphene oxide
Nanosheet
Bath ultrasound

ABSTRACT

For the first time, this work reports a facile sonochemical route in the synthesis of graphene oxide nanosheets (GO) via oxidation of graphite (G). The synthesis of GO was carried out in a fast way under ultrasonic bath irradiation (GO-U). In comparison, the synthesis of GO via classical method (GO-C) was done under the same conditions as ultrasonic method. The products were completely different and the oxidation did not happen the same as way as ultrasonic method. Furthermore, GO was synthesized based on classical approach that most commonly used (GO-C′), not under the same conditions as ultrasonic method. The GO sheets were characterized using UV–Vis, Fourier transform infrared (FT-IR), X-ray diffraction (XRD), transmission electron microscope (TEM), thermal gravimetry (TG), and Raman spectroscopy techniques. The XRD confirms that the spaces between GO-U and GO-C′ sheets were higher than graphite. Also, XRD indicated that the GO-U has fewer sheets rather than GO-C′. The TEM observations were confirmed the synthesis of nanosheets. The UV–Vis results were shown the absorption peaks at 230 nm for GO-U and GO-C′, at 245 nm for GO-C, and at 255 nm for G. The blue shift in GO-U with respect to G and GO-C can be interpreted based on the higher character of sp^3/sp^2 in GO-U than G and GO-C. The FT-IR presents the oxygenated functional groups on graphene oxide sheets. A reduction in size of the in-plane sp^2 domains was observed by Raman spectrum. The BET analysis for G, GO-U and GO-C′ confirmed that GO-U has a highest specific surface area among all the samples. Therefore, the ultrasonic bath method even with low intensity has a fundamental role in the synthesis of graphene oxide nanosheets and it is relatively fast, simple, cost-effective and efficient as compared to the classical method.

1. Introduction

Graphene is a planar monolayer of carbon atoms that arranged into a two-dimensional honeycomb lattice with sp^2 hybridized and a carbon–carbon bond length of 0.142 nm [1–5]. Graphene is a basic building block of graphitic materials for all dimensionalities. It can be wrapped up into 0D fullerene, rolled into 1D nanotube or stacked into 3D graphite [5–8]. This unique structure endows graphene with various superior properties, including excellent thermal conductivity (5300 W/mK), mechanical properties (Young's modulus ~ 1100 GPa), mobility of charge carriers electrical (~2000 S/cm), specific magnetism and large surface area (~2630 m^2/g) [1,9–12]. Graphene is often categorized by the number of stacked layers: single layer, few-layer (2–10 layers), and multi-layer. Ideally, for preserving the distinct properties of the graphene, its use should be narrowed to single or few-layer morphology. Nonetheless, advantageous properties can still be observed in thin graphite form [13]. For example few layers graphene demonstrated outstanding potential ability for flexible photovoltaic applications [14]. Totally, these properties attract great scientific attention during recent years in various fields, such as solar cells [15], sensors [16], super-capacitors [17], transparent electrodes [18], energy storage [19] and nanocomposites [20,21]. Specifically, on the basis of its chemical properties, large surface area, unique mesoporous surface and geometry, graphene and chemically modified graphene (like GO) are promising candidates for several applications such as antibacterial and photocatalytic activities.

GO has a rich assortment of oxygen-containing groups including carboxyl, hydroxyl, and epoxide that appeared on the surface of exfoliated graphene sheets [22]. GO is a single-atom-thick sheet that arranged by localized sp3 defects within the sp^2-bonded carbon atoms in a hexagonal lattice with two-dimensional planar

* Corresponding author at: Sonochemical Research Center, Department of Chemistry, Ferdowsi University of Mashhad, 91775 Mashhad, Iran. Fax: 0098 511 8795457.
E-mail address: moh_entezari@yahoo.com (M.H. Entezari).

http://dx.doi.org/10.1016/j.jcis.2014.06.055
0021-9797/

sheets. It has recently received considerable attentions as a novel derivative of graphene. The presence of oxygen functional groups on the GO makes considerable potential in fabricating various graphene-based composites. Reversibly, the functional groups on the GO can be reduced to graphene by chemical, photochemical, photothermal, and sonochemical reduction methods [22,23].

GO is considered as promising materials for different applications owing to its excellent aqueous processability, amphiphilicity, surface functionalizability, surface enhanced Raman scattering (SERS) property, and fluorescence quenching ability [24]. These fascinating properties of GOs are mainly derived from its unique chemical structures composed of small sp^2 carbon domains surrounded by sp^3 carbon domains and oxygen containing hydrophilic functional groups. Therefore, GO has been applied intensively into inorganic or organic hybrid nanocomposite systems [24,25].

Various methods have been used to synthesize graphene oxide. Up to now, the most popular method employed for the synthesis of graphene oxide is chemical oxidation of graphite (Hummer's method). This method involves oxidation of graphite to GO using highly oxidizing reagents such as potassium permanganate ($KMnO_4$) and sulfuric acid (H_2SO_4) [26]. However, the graphene oxide prepared by this method requires long time and high temperatures. In sonication method, in addition of reducing the time and temperature of the process, the product (GO-U) has more interesting properties than GO-C and GO-C′.

Recently, sonochemical method becomes more promising in the synthesis of several kinds of nanomaterials. The mechanism of sonochemistry is based on the acoustic cavitation phenomenon that involves formation, growth, and collapse of the bubbles in liquid medium. According to the hot spot theory, extremely high temperature about 5000 K, very high cooling rate about 10^{10} Ks^{-1} and high pressure about 20 MPa arises during the acoustic cavitation. Thus, the critical conditions produced during the cavitation process result in unique properties of the synthesized nanoparticles. The sonochemical method can be more suitable for the synthesis of GO that requires extreme conditions which generally not accessible in the conventional synthesis methods [27–29].

In this work, we have attempted to synthesize GO nanosheets via facile sonochemical method (Fig.1) for the first time. Besides being facile, our process has several advantages like low processing temperature, short reaction time, and having GO with few layers in comparison with classical techniques.

2. Experimental

2.1. Materials and methods

Graphite powder (purity 99%, mesh 325), potassium permanganate ($KMnO_4$), sodium nitrate ($NaNO_3$), sulfuric acid (H_2SO_4), hydrochloric acid (HCl), and hydrogen peroxide (H_2O_2) were obtained from Merck and used without further purification. Deionized water (DI) was used in the synthesis of the GO. The Hummer's method with some modifications was applied for the synthesis of GO nanosheets.

2.2. Synthesis of graphene oxide

In a typical procedure, 0.5 g graphite and 0.5 g $NaNO_3$ were added into 23 mL H_2SO_4. The mixture was stirred in an ice bath. Then, to keep the temperature of the suspension lower than 20 °C, 3.0 g $KMnO_4$ was gradually added. After that, the suspension was placed in ultrasonic bath and irradiated for 20 min at room temperature (this step last 2 h at 35 °C in classical method). Then, the prepared suspension was diluted by 40 mL de-ionized water (in classical method the suspension at this step was stirred for long time ~ 5 days at high temperature, 98 °C [30]). Under ultrasound, the long step mentioned in classical method was not applied. Finally, 100 mL DI water with 3 mL H_2O_2 (30%) was added to the suspension in order to reduce residual permanganate to soluble manganese ions, corresponding to stopping the gas evolution of the suspension. The color of the solution changed from dark brown to yellow (Fig. 2b). The mixture was filtered and washed with HCl aqueous solution 1:10 (250 mL) to remove metal ions followed by washing with distilled water to remove the acid. The resulting solid was dried under vacuum at 80 °C for 24 h (GO-U). The procedure was repeated without ultrasonic irradiation (classical method) under the same conditions as ultrasonic method for preparing GO-C (Fig. 2a). Furthermore, GO was synthesized based on classical approach that most commonly used [30], not under the same conditions as ultrasonic method (GO-C′).

2.3. Characterization and equipment

The structure, morphology, and optical properties of the as-prepared nanosheets were characterized by XRD, FTIR, Raman, TEM, UV–Vis and thermal gravimetry analysis (TGA). The XRD was performed in a wide range angle (2θ = 0–60°) by Bruker-axs, D8 Advance model at a scanning rate of 0.04°/s, with monochromatized Cu Kα radiation (λ = 1.5406 Å). The TEM measurements were carried out by Philips CM120 120 kV. The optical properties of the GO were obtained by UV–Vis spectroscopy (Unico 2800). Raman spectroscopy was performed with an Almega Thermo Nicolet Dispersive Raman Spectrometer with a 532 nm laser excitation. TGA was conducted with STA503 that was fitted to Ar gas flow on sample size 8 mg, and the mass was recorded as a function of temperature. The samples were heated from room temperature to 600 °C at 5 °C/min. FTIR were recorded on a Thermo Nicolet 370 spectrometer, the spectrum was obtained by mixing the sample with

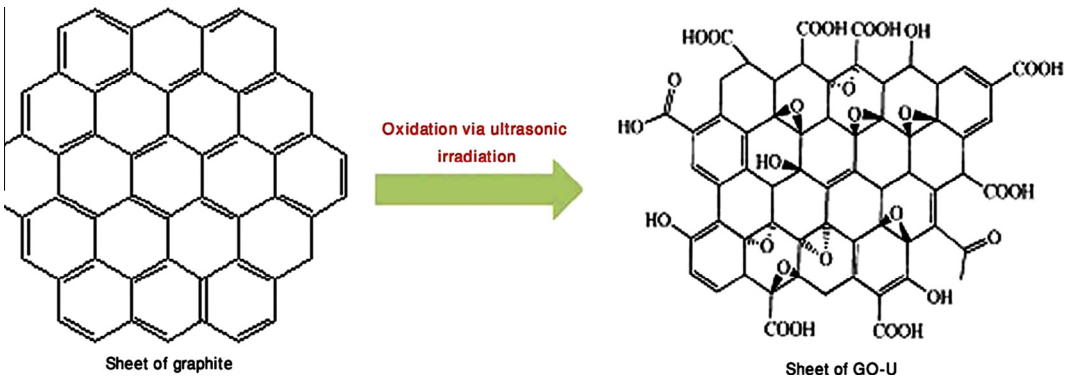

Fig. 1. Schematic view of GO synthesis.

Fig. 2. Pictures of the as-prepared GO-U and GO-C under the same conditions.

KBr. The specific surface area of the samples were measured with a surface area analyzer (JW-K) through BET method.

3. Results and discussion

3.1. FTIR spectroscopy

Fig. 3 shows FTIR spectra of graphite (G) and the as-prepared graphene oxide via ultrasound (GO-U) and classical (GO-C) and (GO-C′) methods. As shown in Fig. 3, for GO-U and GO-C′, the peak at 3395.23 cm^{-1} and 3423.89 cm^{-1}, belongs to stretching vibrations of hydroxyl groups which is related to the adsorbed water and water in or between graphene interlayer. The stretching vibrations of C═O and C—O functional groups for GO-U and GO-C′ were detected clearly at 1715.78 cm^{-1} , 1717.11 cm^{-1} and 1045.63 cm^{-1}, 1049.74 cm^{-1}, respectively. The peak located at 1227.48 cm^{-1} and 1215.61 cm^{-1} for GO-U and GO-C′ are most often related to the vibration of epoxy group. These carboxyl and epoxy groups indicate that the original extended conjugated π-orbital system of the natural graphite was destroyed and the oxygen-containing groups were inserted into carbon skeleton during the oxidation of graphite powder. The spectrum of GO-U and GO-C′ also show a C═C peak at 1584.62 cm^{-1} and 1583.53 cm^{-1} corresponding to the remaining sp^2 character [31,32]. The mentioned peaks do not appear in the spectrum of graphite except the obvious peak around 3519.76 cm^{-1} which assigned to the stretching vibration of hydroxyl group. This indicates that graphite adsorb water too. The polar groups, especially the hydroxyl groups, make it easy to form hydrogen bond not only between GO layers but also between GO and water molecules. Therefore, the GO-U and GO-C′ exhibited the hydrophilic property. The FTIR spectrum of GO-C shows low intensity peaks at 1719.86 cm^{-1}, 1568.67 cm^{-1}, and 1219.04 cm^{-1} that indicates the partial oxidation of graphite powder can occur in classical method under the same conditions as ultrasonic method.

3.2. UV–Vis analysis

More evidences came from UV–Vis spectroscopy. The UV–Vis spectra of the G, GO-C, GO-U and GO-C′ were shown in Fig.4. The UV–Vis spectrum of carbon particles usually exhibits a broad peak (π–π^*) due to sp^2 hybridization which appears in the range of 200–

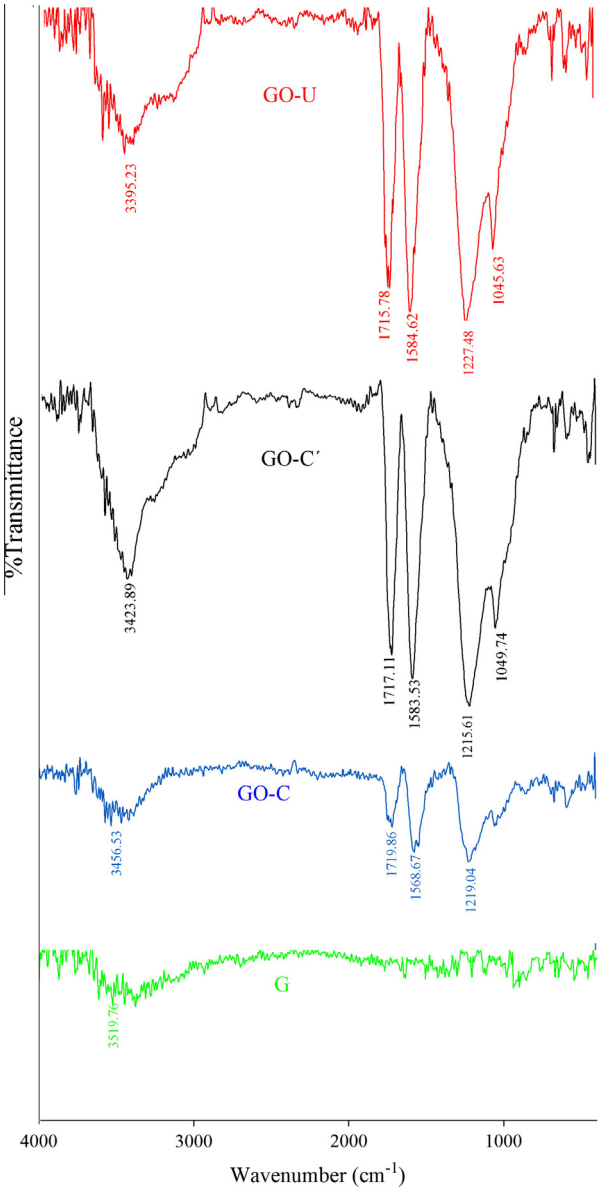

Fig. 3. FTIR spectra of GO-U, GO-C′, GO-C and G.

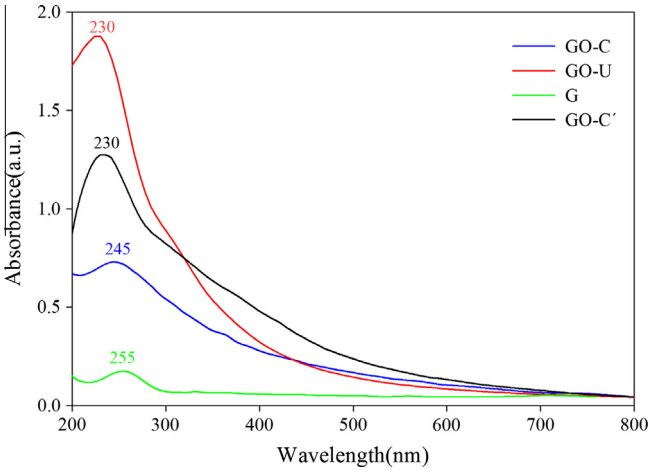

Fig. 4. UV–Vis absorption spectra of the aqueous dispersions of GO-U, GO-C′, GO-C and G.

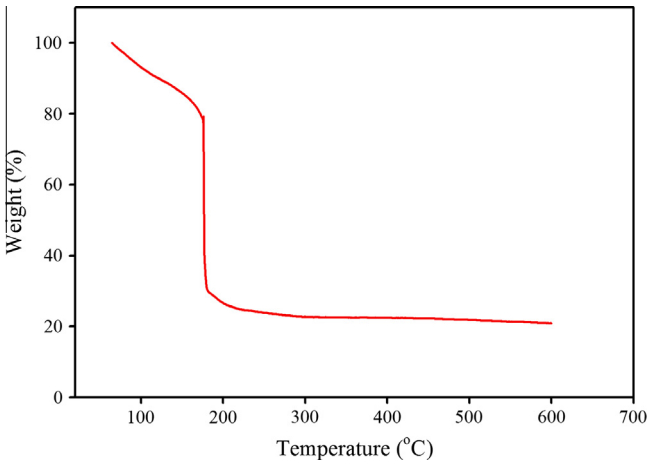

Fig. 5. TGA plot for GO-U.

300 nm. In principle, the (π–π^*) band position of carbon-based material should be merely related to the sp^2/sp^3 character. In particular, it has been assessed that the (π–π^*) band position shifts toward the visible as the sp^2 character increases and the growth of the graphene sp^2 layers occurs [33]. Therefore, in the case of GO-U and GO-C′, the value of sp^2 due to the presence of oxygen-containing functional groups should be lower than that of graphite and the peak position should be shifted toward lower wavelengths. Our results in Fig. 4 confirm the mentioned claim.

As shown in Fig. 4, the spectrum of GO-U and GO-C′ show a sharp absorption peak at 230 nm attributed to the π–π^* of the C=C in the rings. A shoulder is also observed around 300 nm, assigned to n–π^* transitions of C=O bonds [34]. The graphite and graphene oxide prepared via classical method show broad and low intensity peak at 245 and 255 nm, respectively. As we expect, by increasing the sp^3 character, the peak position shifted to the smaller wavelength in GO-U and furthermore it is not possible to oxidize graphite in classical method (GO-C) the same as ultrasonic method (GO-U) sample. This could be attributed to the collapse of the cavity which resulted to the harsh conditions in medium of reaction and facilitated the synthesis of GO.

3.3. Thermal gravimetry analysis

The presence of the oxygen functional groups makes GO thermally unstable, as it undergoes pyrolysis at elevated temperatures. The thermal behavior of the GO-U was investigated by TGA. As shown in Fig 5, it exhibits about 10% mass loss below 100 °C resulting from the removal of adsorbed water. The sharp mass loss (about 80%) at 177 °C would be mainly due to the decomposition of oxygen-containing groups and the loss of interlayer water molecules. The pyrolysis of the labile oxygen-containing functional groups can be led to CO, CO_2 and steam.

3.4. XRD analysis

The crystalline structures of graphite and graphene oxide can be evaluated by XRD. The feature diffraction peak for both graphite and graphene oxide is related to the stacking order. As shown in Fig. 6a, graphite shows an intense peak (002) at 26.48°, whereas the feature diffraction peak of GO-C′ and GO-U appears at

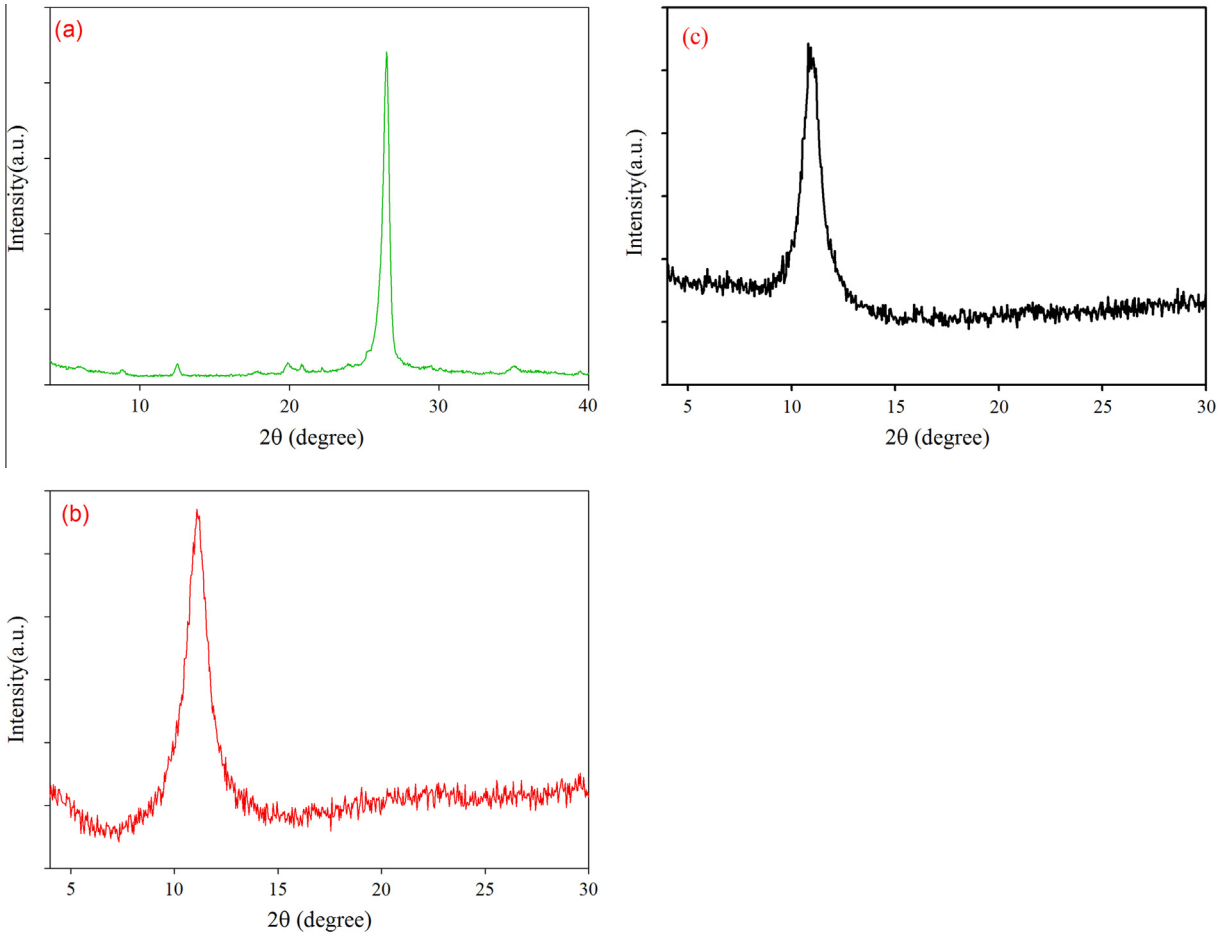

Fig. 6. X-ray diffraction patterns of (a) G, (b) GO-U and (c) GO-C′.

Table 1
Characteristics of GO-U and GO-C′ by XRD.

Sample	2θ (°)	FWHM (°)	d (nm)	D (nm)	Number of layers
GO-U	11.10	1.20	0.795	6.57	8.26
GO-C′	10.80	1.01	0.806	7.81	9.69

$2\theta = 10.80°$ and $2\theta = 11.10°$, respectively (Fig. 6b and c). The interlayer distance of the graphite was 3.36 Å and it was increased to 7.95 Å and 8.06 Å for GO-U and GO-C′, respectively. The oxidation of graphite is accompanied by the increase of the interlayer distance (d-spacing), indicating the presence of intercalated H_2O molecules and attachment of various oxide groups between the layers. Using the Scherrer equation, the number of layers in the sample can be obtained from the corresponding line broadening by Lorentzian fitting of the reflection. The diffraction angle (2θ), interlayer distance (d), full width at half-maximum (FWHM), the mean crystallite diameter (D), and the average number of sheets in crystallite (N) are collected in Table 1. It can be seen that the number of layers is about 8, while the number of GO layers by classical method is about 10 layers. This indicates that sonication method led to fewer layers of graphene oxide and can be considered as superiority with respect to classical one.

3.5. Raman spectroscopy

The G and GO samples were studied by Raman spectroscopy too. This method is a versatile and non-destructive characterization technique for studying the structure, defect levels and crystallinity. Typically, the Raman spectrum of the graphite shows the in-phase vibration of the graphite lattice (G band) at 1579 cm^{-1} and a weak D band at 1350 cm^{-1} (Fig. 7a). As shown in Fig. 7b and c, the Raman spectrum for GO-C′ and GO-U presents a broadened G band at 1598 cm^{-1} and 1590 respectively, owing to the presence of isolated double bonds that resonate at higher frequencies than the G band of graphite. The G line was related to the first-order scattering of the E_{2g} phonons of sp^2 carbon atoms. The D band of GO-U and GO-C′ becomes evident at 1354 cm^{-1}, and 1350 cm^{-1}, indicating the reduction in size of the in-plane sp^2 domains due to the extensive oxidation. The D line as a breathing mode of κ-point phonons of A_{1g} symmetry is assigned to structural imperfections induced by the attachment of hydroxyl and/or epoxide groups on the carbon surface [35]. The intensity ratio of the D and G peak has been used as a metric of disorder in graphene oxide, such as arising from ripples, edges, charged impurities, presence of domain boundaries, and others. It is noteworthy that the D/G intensity ratio of GO-U is 1.01, in comparison with the value of 0.78 for graphite and 0.95 for GO-C′. The increase in the ratio indicates a decrease in the size of the in-plane sp^2 domains and a partially ordered crystalline structure of GO-U compared to G and GO-C′ [36].

The Raman could be used to distinguish the quality of graphene and graphene oxide and to determine the number of layers for n-layer graphene (for n up to 5) by the shape, width, and position of the 2D peak [34]. Single-layer graphene sheets have a single, sharp 2D peak below 2700 cm^{-1}, while bilayer sheets have a broader and upshifted 2D peak located at ~2700 cm^{-1}. Sheets with more than five layers and bulk graphite exhibit similar spectra and the 2D peaks are upshifted to positions greater than 2700 cm^{-1}. Totally, the 2D peak shifts to higher wavenumber values and

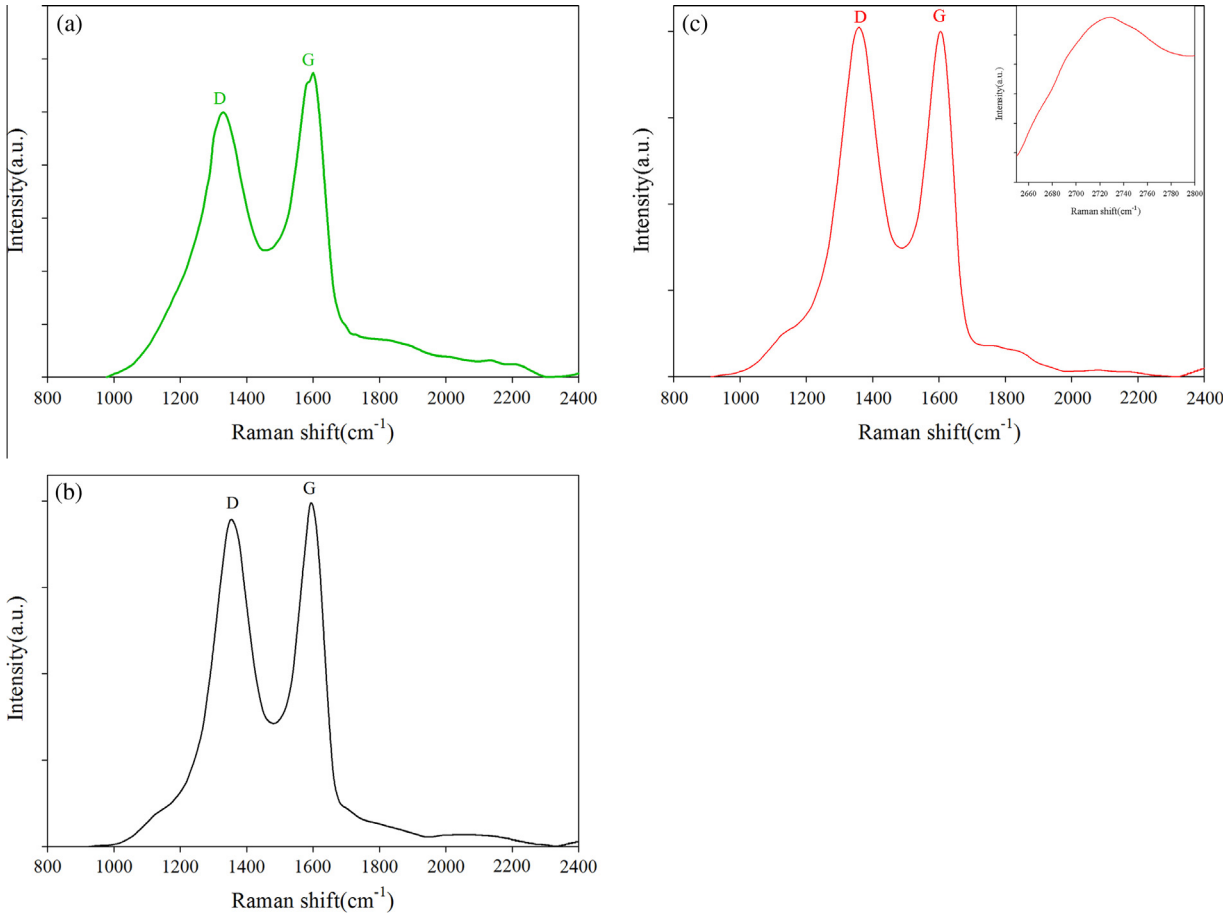

Fig. 7. Raman spectrum of (a) G, (b) GO-C′ and (c) GO-U (inset: 2D peak).

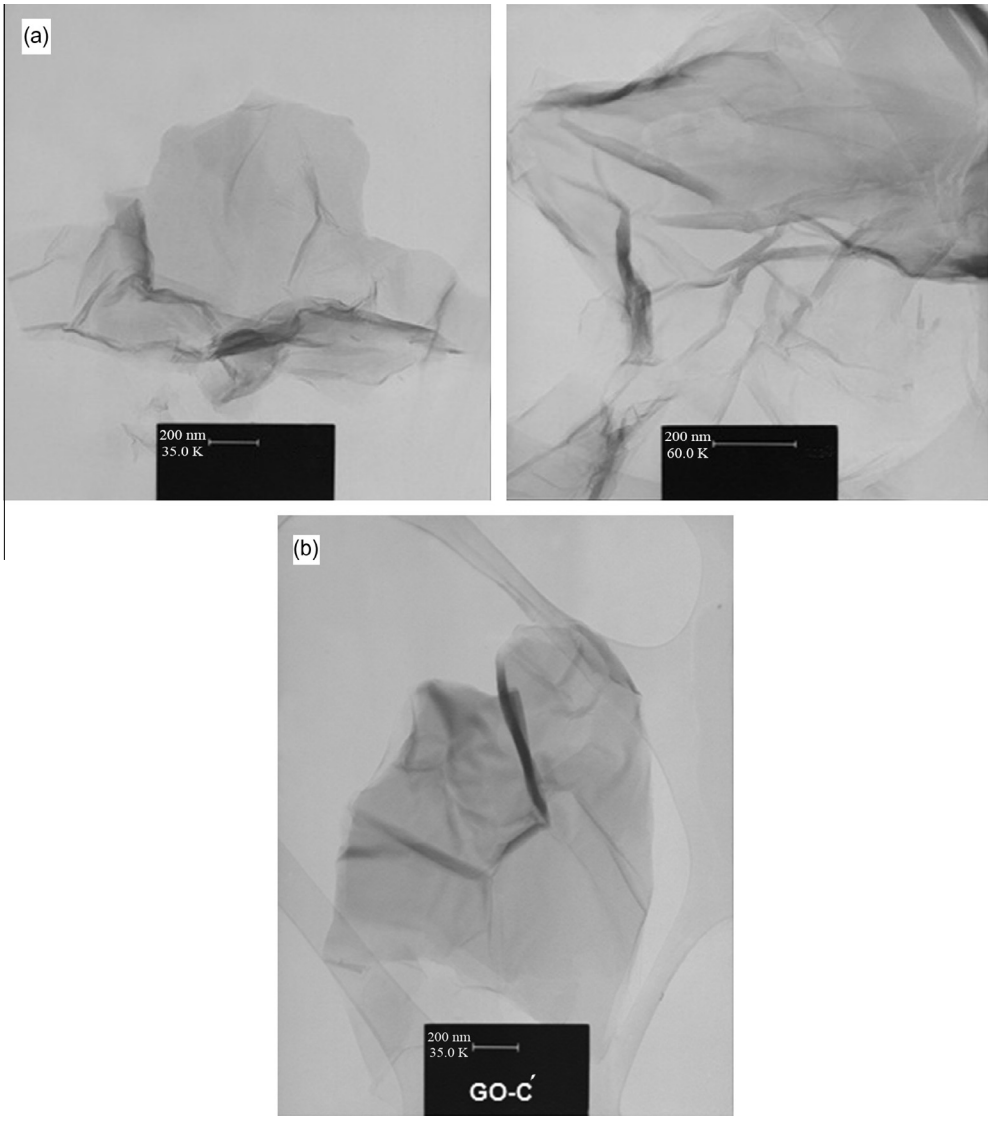

Fig. 8. TEM images of (a) GO-U and (b) GO-C′.

becomes broader for an increasing number of layers. As shown in inset Fig. 7c, a broad 2D peak at larger than 2700 cm^{-1} indicates that the number of layers is more than five which is in agreement with XRD analysis.

3.6. TEM analysis

In order to obtain the structure and morphology of our graphene oxide sheets synthesized by ultrasound and classical methods, we focused on the TEM observation. Fig. 8 shows the TEM images of the as-prepared GO-U and GO-C′ that well indicates a sheet structure in sonication method as well as classical method. The sheets are not perfectly flat and show intrinsic microscopic roughness. The transparent and creased GO sheets have exhibited mono-or few layer planar sheet and the size of the flakes are above 200 nm in both samples.

3.7. BET surface area

The surface area measurement using the BET method by nitrogen gas adsorption was done for the samples of G, GO-C′ and GO-U. Fig. 9 compares the specific surface area of all samples. GO-U has an obvious increase of specific surface area near 20 times with respect to G. This is corresponding to the formation of oxygen-containing groups such as carbonyl and hydroxyl in the graphite layer during the oxidation process. Comparing the BET results of GO-C′ and GO-U shows that the specific surface area of GO-U is more

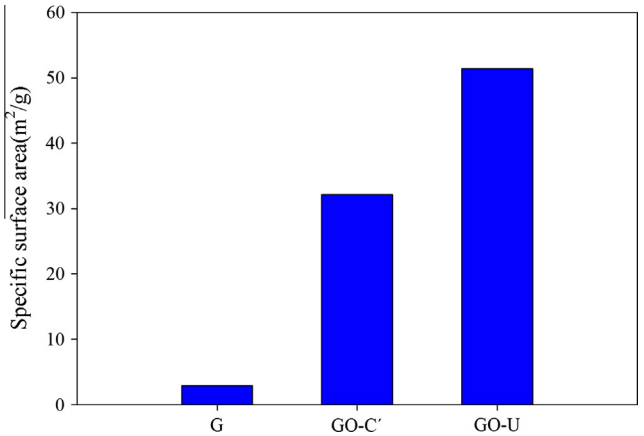

Fig. 9. Specific surface area of G, GO-U and GO-C′.

than GO-C′ (1.5 times larger), resulting from more oxygen-containing groups such as epoxy and hydroxyl were introduced on or between the layers. The specific surface area is related to the number of graphene oxide layers. Fewer layers showed larger specific surface area [19]. As can be seen from the results obtained, the oxidation of graphite was enhanced with using ultrasonic irradiation in the synthesis of GO. The fully oxidation easily causing configuration changed from a planar sp^2-hybridized to a distorted sp^3-hybrized geometry. More oxygen-containing groups such as epoxy and hydroxyl are introduced on or between the layers [19].

4. Conclusion

For the first time, a facile sonochemical method is reported in the synthesis of graphene oxide nanosheets. UV–Vis, Raman, FT-IR, thermal gravimetry, and TEM analysis confirm the formation of graphene oxide nanosheets very well. In addition, the number of layers in GO-U is lower than GO-C′ and G. The BET measurements also confirm that the GO-U has a larger surface area than GO-C′ and G samples. Harsh conditions of ultrasonic irradiation are responsible for the synthesis of GO-U with higher surface area which has significant effect in several applications. This method is fast, simple, effective and economic. This new method may become a promising way for preparation of graphene oxide due to its wide applications in various areas.

Acknowledgment

The support of Ferdowsi University of Mashhad (Research and Technology) for this work (code 3/29791, date 2014/01/26) is appreciated.

References

[1] H. Wang, X. Yuan, Y. Wu, H. Huang, X. Peng, G. Zeng, H. Zhong, J. Liang, M. Ren, Adv. Colloid Interface Sci. 195–196 (2013) 19–40.
[2] A. Reina, X. Jia, J. Ho, D. Nezich, H. Son, V. Bulovic, M.S. Dresselhaus, J. Kong, Nano Lett. 9 (2009) 30–35.
[3] M. Bala Murali Krishna, N. Venkatramaiah, R. Venkatesan, D. Narayana Rao, J. Mater. Chem. 22 (2012) 3059–3068.
[4] Z. Sun, D.K. James, J.M. Tour, J. Phys. Chem. Lett. 2 (2011) 2425–2432.
[5] .T. Kuila, S. Bose, A. Kumar Mishra, P. Khanra, N.H. Kim, J.H. Lee, Progr. Mater. Sci. 57 (2012) 1061–1105.
[6] S. Vadukumpully, J. Paul, S. Valiyaveettil, Carbon 47 (2009) 3288–3294.
[7] X. Su, G. Wang, W. Li, J. Bai, H. Wang, Adv. Powder Technol. 24 (2013) 317–323.
[8] B. Zhang, X. Zheng, H. Li, J. Lin, Anal. Chim. Acta 784 (2013) 1–17.
[9] S. Park, R.S. Ruoff, Nat. Nanotechnol. 4 (2009) 217–224.
[10] L. Tang, X. Li, D. Du, C. He, Progr. Nat. Sci. Mater. Int. 22 (2012) 341–346.
[11] .M. Terrones, A.R. Botello-Méndez, J. Campos-Delgado, F. López-Uríasd, Y.I. Vega-Cantú, F.J. Rodríguez-Macías, A. Laura Elías, E. Mu~noz-Sandoval, A.G. Cano-Márquez, J. C Charlier, H.Terrones, Nano Today 5 (2010) 351–372.
[12] A. Almazan, Cosmos 8 (2012) 1–18.
[13] M.S. Artiles, C.S. Rout, T.S. Fisher, Adv. Drug Deliv. Rev. 63 (2011) 1352–1360.
[14] H.P. Huang, J.J. Zhu, Chinese J. Anal. Chem. 39 (7) (2011) 963–971.
[15] Z.K. Liu, J.H. Li, Z.H. Sun, G.A. Tai, S.P. Lau, F. Yan, Acs Nano 6 (2012) 810–818.
[16] P. Kailian Ang, W. Chen, A. Thye, S. Wee, K. Ping Loh, J. Am. Chem. Soc. 130 (2008) 14392–14395.
[17] X. Li, T. Zhao, Q. Chen, P. Li, K. Wang, M. Zhong, J. Wei, D. Wu, B. Wei, H. Zhu, Phys. Chem. Chem. Phys. 15 (2013) 17752–17757.
[18] L. Zhao, L. Zhao, Y. Xu, T. Qiu, L. Zhi, G. Shia, Electrochim. Acta 55 (2009) 491–497.
[19] X. Tong, H. Wang, G. Wang, L. Wan, Z. Ren, J. Bai, J. Bai, J. Solid State Chem. 184 (2011) 982–989.
[20] Q. Zhuo, Y. Ma, J. Gao, P. Zhang, Y. Xia, Y. Tian, X. Sun, J. Zhong, X. Sun, Inorg. Chem 52 (2013) 3141–3147.
[21] L. Zheng, D. Ye, L. Xiong, J. Xu, K. Tao, Z. Zou, D. Huang, X. Kang, S. Yang, J. Xia, Anal. Chim. Acta 768 (2013) 69–75.
[22] Q. Xiang, J. Yu, M. Jaroniec, Chem. Soc. Rev. 41 (2012) 782–796.
[23] G. Eda, M. Chhowalla, Adv. Mater 22 (2010) 2392–2415.
[24] C. Chung, Y.K. Kim, D. Shin, S.R. Ryoo, B.H. Hong, D.H. Min, Acc. Chem. Res. 46 (10) (2013) 2211–2224.
[25] D.L. Han, L.F. Yan, W.F. Chen, W. Li, Carbohyd. Polym 83 (2011) 653–658.
[26] D.R. Dreyer, S. Park, C.W. Bielawski, R.S. Ruoff, Chem. Soc. Rev 39 (2010) 228–240.
[27] H. Xu, B.W. Zeiger, K.S. Suslick, Chem. Soc. Rev 42 (2013) 2555–2567.
[28] C. Deng, H. Hub, X. Ge, C. Han, D. Zhao, G. Shao, Ultrason. Sonochem. 18 (2011) 932–937.
[29] V. Safarifard, A. Morsali, Ultrason. Sonochem 19 (2012) 823–829.
[30] J. Chen, X. Cui, Q. Wang, H. Wang, X. Zheng, C. Liu, T. Xue, S. Wang, W. Zheng, J. Colloid Interface Sci. 383 (2012) 140–147.
[31] Y. Dong, J. Li, L. Shi, J. Xu, X. Wang, Z. Guo, W. Liu, J. Mater. Chem. A 1 (2013) 644–650.
[32] T. Yang, L.H. Liu, J.W. Liu, M.L. Chen, J.H. Wang, J. Mater. Chem 22 (2012) 21909–21916.
[33] .C. Russo, F. Stanzione, M. Alfè, A. Ciajolo, A. Tregrossi, Spectral analysis in the UV-visible range for revealing the molecular form of combustion generated carbonaceous species, MCS7 (2011) 1–10.
[34] J. Shen, M. Shi, H. Ma, B. Yan, N. Li, Y. Hu, M. Ye, J. Colloid Interface Sci. 351 (2010) 366–370.
[35] Y. Zhu, S. Murali, W. Cai, X. Li, J.W. Suk, J.R. Potts, R.S. Ruoff, Adv. Mater 22 (2010) 3906–3924.
[36] X. Meng, D. Geng, J. Liu, M. Norouzi Banis, Y. Zhang, R. Li, X. Sun, Non-aqueous approach to synthesize amorphous/crystalline metal oxide-graphene nanosheet hybrid composites, J. Phys. Chem. C. 114 (2010) 18330–18337.